AMERICAN SOCIETY FOR MICROBIOLOGY | Infection and Immunity®

CELLULAR MICROBIOLOGY:
PATHOGEN-HOST CELL MOLECULAR INTERACTIONS

The Autotransporter IcsA Promotes *Shigella flexneri* Biofilm Formation in the Presence of Bile Salts

Volkan K. Köseoğlu,[a] Chelsea P. Hall,[a] Eric M. Rodríguez-López,[b] Hervé Agaisse[a]

[a]Department of Microbiology, Immunology, and Cancer Biology, University of Virginia School of Medicine, Charlottesville, Virginia, USA
[b]Department of Biology, University of Puerto Rico at Ponce, Ponce, Puerto Rico, USA

ABSTRACT *Shigella flexneri* is an intracellular bacterial pathogen that invades epithelial cells in the colonic mucosa, leading to bloody diarrhea. A previous study showed that *S. flexneri* forms biofilms in the presence of bile salts, through an unknown mechanism. Here, we investigated the potential role of adhesin-like autotransporter proteins in *S. flexneri* biofilm formation. BLAST search analysis revealed that the *S. flexneri* 2457T genome harbors 4 genes, *S1242*, *S1289*, *S2406*, and *icsA*, encoding adhesin-like autotransporter proteins. Deletion mutants of the *S1242*, *S1289*, *S2406* and *icsA* genes were generated and tested for biofilm formation. Phenotypic analysis of the mutant strains revealed that disruption of *icsA* abolished bile salt-induced biofilm formation. IcsA is an outer membrane protein secreted at the bacterial pole that is required for *S. flexneri* actin-based motility during intracellular infection. In extracellular biofilms, IcsA was also secreted at the bacterial pole and mediated bacterial cell-cell contacts and aggregative growth in the presence of bile salts. Dissecting individual roles of bile salts showed that deoxycholate is a robust biofilm inducer compared to cholate. The release of the extracellular domain of IcsA through IcsP-mediated cleavage was greater in the presence of cholate, suggesting that the robustness of biofilm formation was inversely correlated with IcsA processing. Accordingly, deletion of *icsP* abrogated IcsA processing in biofilms and enhanced biofilm formation.

KEYWORDS IcsA, *Shigella flexneri*, actin, autotransporter, bile, biofilm, cholic acid, deoxycholic, dissemination

A recent global estimation marks *Shigella* spp. as the second leading cause of diarrheal deaths among all age groups, the leading cause of diarrheal deaths among adults aged 15 to 99 years, and the main etiology, along with rotavirus and *Cryptosporidium* spp., responsible for diarrheal deaths of children under 5 years of age (1). *Shigella* species such as *S. flexneri*, *S. sonnei*, *S. dysenteriae*, and *S. boydii* are enteric bacterial pathogens showing different epidemiologies worldwide (2). *S. flexneri* is primarily responsible for infections in developing countries, while *S. sonnei* causes the majority of infections in industrialized countries (3, 4). *Shigella*-associated diarrhea, also known as bacillary dysentery or shigellosis, can occur after the ingestion of as few as 10 to 100 bacteria and is mostly spread via the fecal-oral route (5, 6). The characteristic symptom of human shigellosis is the presence of blood and mucus in stool, which correlates with acute destruction of the colonic epithelium and a massive immune response (7).

Shigella spp. are intracellular pathogens that invade colonic epithelial cells, multiply in the cytosol of these cells, and spread to adjacent cells (8). The pathogenic properties of *Shigella* spp. rely on a large virulence plasmid that harbors genes encoding the structural components of the type 3 secretion system (T3SS), effector proteins injected into host cells by the T3SS, chaperones, and transcription factors controlling the

Citation Köseoğlu VK, Hall CP, Rodríguez-López EM, Agaisse H. 2019. The autotransporter IcsA promotes *Shigella flexneri* biofilm formation in the presence of bile salts. Infect Immun 87:e00861-18. https://doi.org/10.1128/IAI.00861-18.

Editor Craig R. Roy, Yale University School of Medicine

Address correspondence to Hervé Agaisse, hfa5y@virginia.edu.

Received 4 December 2018
Returned for modification 14 January 2019
Accepted 9 April 2019
Accepted manuscript posted online 15 April 2019
Published 20 June 2019

expression of virulence genes (9, 10). Both bacterial and cellular factors involved in each step of *Shigella* species pathogenesis have been extensively studied, especially using *S. flexneri* as a model in different cell lines (11). However, it remains elusive how *S. flexneri* withstands adverse conditions and colonizes specific niches along the intestinal tract.

Upon ingestion, *S. flexneri* encounters multiple hurdles before reaching the colonic epithelium. Some of these challenges include high stomach acidity, gut microbiota, physical mucus barrier, and host production of antimicrobial peptides, proteases, and bile salts (12). Bile salts or sodium salts of bile acids are organic components of bile, which is a host secretion produced in the liver and stored in the gallbladder. Following food intake, bile is secreted into the small intestine and facilitates the absorption of lipids and fat-soluble vitamins (13). Chenodeoxycholic acid and cholic acid are the primary bile acids synthesized from cholesterol and subsequently conjugated to glycine and taurine in humans (14). Bacterial hydrolases and dehydrogenases convert these primary bile salts to secondary bile salts, which are predominantly deoxycholic acid and lithocholic acid in the colon (15, 16).

The amphipathic structure of bile salts, which provides detergent-like properties, confers antimicrobial activity by compromising bacterial membrane integrity and permeability (13). However, certain bacterial pathogens, including *Shigella* spp., can exploit bile salts as cues to adjust virulence traits (17, 18). Previous reports revealed that bile salts modulate *Shigella* species interaction with its environment. Pope et al. first reported that growth in the presence of the secondary bile salt deoxycholate (DOC) enhanced *S. flexneri* and *S. dysenteriae* adhesion to HeLa cells, which relied on the presence of the virulence plasmid (19). Subsequently, Faherty et al. reported that exposure to bile salts increased *S. flexneri* adherence to polarized intestinal T84 cells (20). Those authors proposed that the *ospE1* and *ospE2* genes are upregulated in the presence of DOC and cholate (CA) and function as adhesins upon outer membrane localization (20). IcsA is another factor found to promote hyperadhesiveness and invasion upon DOC exposure in a T3SS-dependent manner (21). Furthermore, DOC was shown to facilitate the association of IpaB-IpaD at the tip of the T3SS needle, which is implicated in the maturation of the T3SS needle tip complex, by inducing a conformational change in IpaD (22, 23). A recent study by Nickerson et al. also indicated that exposure to a mixture of DOC and CA stimulates biofilm formation by *Shigella* spp. (24), similar to the effect of bile and bile salts (DOC and CA) on other Gram-negative enteric pathogens, such as *Salmonella* (25, 26) and *Vibrio cholerae* (27).

Biofilms are surface-associated dynamic structures developed by single or multiple microbial species embedded in a self-produced extracellular matrix (28). Biofilm formation emerges as an adaptive trait of microorganisms under harsh conditions, as it provides protection for the community from external threats such as antimicrobials and host defense (29, 30). Here, we investigated the involvement of *S. flexneri* adhesin-like autotransporter proteins in bile salt-mediated biofilm formation. We found that IcsA, an essential factor for *S. flexneri* intracellular infection, is critical for extracellular biofilm formation.

RESULTS

Search for potential *Shigella flexneri* biofilm components. Mature biofilms are composed of an extracellular polymeric matrix and bacterial cells encased in the complex matrix network (31). Extracellular DNA, exopolysaccharides, and extracellular proteinaceous structures such as fimbrial surface appendages and nonfimbrial adhesins are common matrix components (32). Nickerson et al. demonstrated that *S. flexneri* displays aggregation and forms biofilms on glass coverslips in the rich medium tryptic soy broth (TSB) when supplemented with bile salts (24). That study also showed an increase in the level of extracellular polymeric substances in these biofilms by using a fluorescein-conjugated lectin which specifically labels polysaccharides (24). We conducted literature and BLAST searches to identify potential *S. flexneri* biofilm components. *Escherichia coli* species are phylogenetically related to *Shigella* spp. (33, 34). Table 1 summarizes the common structures that serve critical functions in different types of

TABLE 1 Common biofilm components produced by *E. coli* but not *S. flexneri*

Component	Function(s) (reference)
Exopolysaccharides	
Cellulose	Interaction with other biofilm components such as curli and flagella that leads to robust architecture and tissue-like property of macrocolonies (70) Integrity of pellicle-type biofilm at air-liquid interface (71) Interaction with curli, encapsulating bacterial cells in a strong shell-like architecture (72)
Poly-*N*-acetylglucosamine	Abiotic surface attachment, cell aggregation, and subsequent biofilm development (73)
Colanic acid	Structural development at later stages of biofilm formation (74)
Capsule	Aggregation leading to development of biofilm-like communities in host cells (75)
Proteinaceous structures	
Flagella	Initial surface contact and early expansion of biofilm (76) Motility required for pellicle-type biofilm formation at air-liquid interface (71)
Curli fibers	Essential structural element of pellicle-type biofilms at air-liquid interface (71) Essential structural component of macrocolonies on agar surface (77) Interaction with cellulose, encapsulating bacterial cells in a strong shell-like architecture (72)
Type 1 fimbriae	Initial surface attachment (76) Integrity of pellicle-type biofilm at air-liquid interface (71) Formation of biofilm-like communities in host cells (78)
Type IV pilus	Microcolony development on abiotic surface under static growth and bacterial aggregation under flow (79)

biofilms developed by pathogenic and nonpathogenic *E. coli* strains. *S. flexneri*, as a host-restricted bacterial pathogen, has undergone a reductive evolution process (also known as pathoadaptation) leading to the inactivation of numerous genes present in *E. coli*, thereby optimizing *S. flexneri* pathogenicity (35). Whether part of pathoadaptation or not, *Shigella* genes involved in the synthesis of different biofilm components (Table 1) are either absent or mutated by various mechanisms.

S. flexneri has lost flagellar motility due to mutations in structural and regulatory genes supporting flagellum biosynthesis (36, 37). Type 1 fimbria biosynthesis was also abolished by an insertion element and a specific nonsense mutation (36, 38). Similarly, the production of curli, which is another fimbrial adhesin, was eliminated in *Shigella* spp. predominantly by insertion elements (39). Employing distinct types of biosynthetic machinery, certain bacterial pathogens synthesize and secrete sugar polymers or exopolysaccharides like cellulose, alginate, poly-*N*-acetylglucosamine, and capsules (40). *S. flexneri* possesses deletions that cause frameshifts in the cellulose synthase genes *bcsA* and *bcsC* (41). Likewise, the large operon in the *S. flexneri* chromosome responsible for colanic acid production also contains pseudogenes, including those encoding colanic acid polymerase (*wcaD*) and glycosyltransferases (*wcaACE*). Moreover, capsular O-antigen (OAg) polysaccharide is not produced by *S. flexneri* due to a frameshift mutation in the corresponding operon, while *S. sonnei* was reported to be capsulated (42). A BLAST search indicated that the operon of poly-*N*-acetylglucosamine biosynthesis was absent in *S. flexneri* as well. Finally, *S. flexneri* lacks genes encoding nonfimbrial biofilm-associated proteins (Baps) secreted by the type I secretion system (43). Thus, we turned our attention to autotransporter proteins, which can operate as nonfimbrial adhesins displayed on the bacterial surface (44).

Autotransporter proteins as potential components of *Shigella* biofilms. Autotransporter proteins, which constitute the type V secretion system, are ubiquitous among bacteria (45). Type Va is the simplest subclass of autotransporter proteins that bear a generic domain organization comprised of an N-terminal signal sequence, a passenger domain, and a translocator domain (46). Following translocation to the periplasm by the Sec machinery, autotransporter proteins interact with chaperones for proper passage through the periplasmic space and then facilitate their own secretion

TABLE 2 *S. flexneri* genes encoding type Va autotransporters

Function/passenger domain	Gene	Pseudogene
Adhesin/AIDA superfamily	*S1242*	*S3194* (*flu*)
	S1289	*S3195* (*flu*)
	S2406	*S2446* (*yfaL*)
	icsA-virG	*S0261* (*yaiT*)
		S0268 (*yaiT*)
		S1246
Protease/immunoglobulin A1 protease family	*S6163* (*sepA*)	
	S4824 (*sigA*)	
	S3178 (*pic*)	

by a translocator or β-barrel domain to the bacterial cell surface with the assistance of outer membrane protein complexes such as the Bam complex (47). Exposed on the bacterial cell surface, the passenger domain of autotransporter proteins can perform different functions, such as adhesion, proteolysis, and interaction with host factors (48).

A BLAST search using the β-barrel domains of homologs (i.e., Aida, antigen 43 [Ag43], TibA, and MisL) in *E. coli* and *Salmonella* species led to the identification of 13 potential autotransporter genes in *S. flexneri* (Table 2). The identified genes encode adhesins and serine proteases, belonging to the Aida superfamily of adhesins and the immunoglobulin A1 protease family, respectively (Table 2). In agreement with the notion of pathoadaptation, 6 genes coding for adhesins in *E. coli* are pseudogenes in *S. flexneri* (Table 2). Our analysis therefore reveals 4 genes, encoding S1242, S1289, S2406, and IcsA, that belong to the Aida superfamily of adhesins and may support *S. flexneri* biofilm formation.

Disruption of *icsA* abrogates bile salt-mediated biofilm formation. We further tested the putative involvement of the identified autotransporters in biofilm formation. We generated deletion mutant strains by inserting a chloramphenicol cassette in *S1242*, *S1289*, *S2406*, or *icsA*, in the *S. flexneri* 2457T genetic background. Strains grew in TSB medium with 0.4% bile salts (TSB-BS), as previously described (24). Biofilm formation was assessed by confocal microscopy, measuring the thickness of biofilms that developed on glass coverslips. While the *S1242*, *S1289*, or *S2406* strain did not show any impairment in biofilm formation, the *icsA* mutant showed a significant decrease (Fig. 1). The defect in biofilm formation observed with the *icsA* mutant was rescued by the expression of a Myc-tagged version of IcsA (IcsA-Myc), which drastically increased biofilm thickness with respect to the wild-type (WT) strain (Fig. 2). These results indicate that IcsA expression is required for bile salt-induced biofilm formation.

IcsA promotes bacterial cell-cell interactions in biofilms. We next utilized the *icsA*/pIcsA-Myc rescue strain to determine IcsA localization in biofilms. After growth in TSB-BS and fixation steps, biofilms were stained with SYTOX and a Myc antibody to visualize *S. flexneri* and IcsA, respectively. As expected, IcsA displayed a polar localization when *S. flexneri* was grown in TSB medium (Fig. 3A, panel I, IcsA-Myc) (49). In the presence of BS, IcsA appeared as large punctae that colocalized with bacterial poles (Fig. 3A, panels II and III, IcsA-Myc). Interestingly, punctae appeared to colocalize with several bacteria in biofilms (Fig. 3A, panels II and III, and see Fig. S1 in the supplemental material). Quantification of these phenotypes indicated that the number of bacteria around a single IcsA-Myc punctum was significantly increased in TSB-BS compared to TSB (Fig. 3B). Collectively, these results suggest that polar IcsA may function as an intercellular adhesin facilitating bacterial cell-cell interactions in bile salt-induced biofilms.

Differential biofilm formation in the presence of DOC and CA. The composition of bile salts varies along the intestinal tract. In healthy human subjects, the level of CA is high in the small intestine, whereas DOC, the dehydroxylated form of CA, is the most abundant bile salt component in the colon (16). We next evaluated the individual contributions of bile salts to *S. flexneri* biofilm formation. The biofilm structures formed

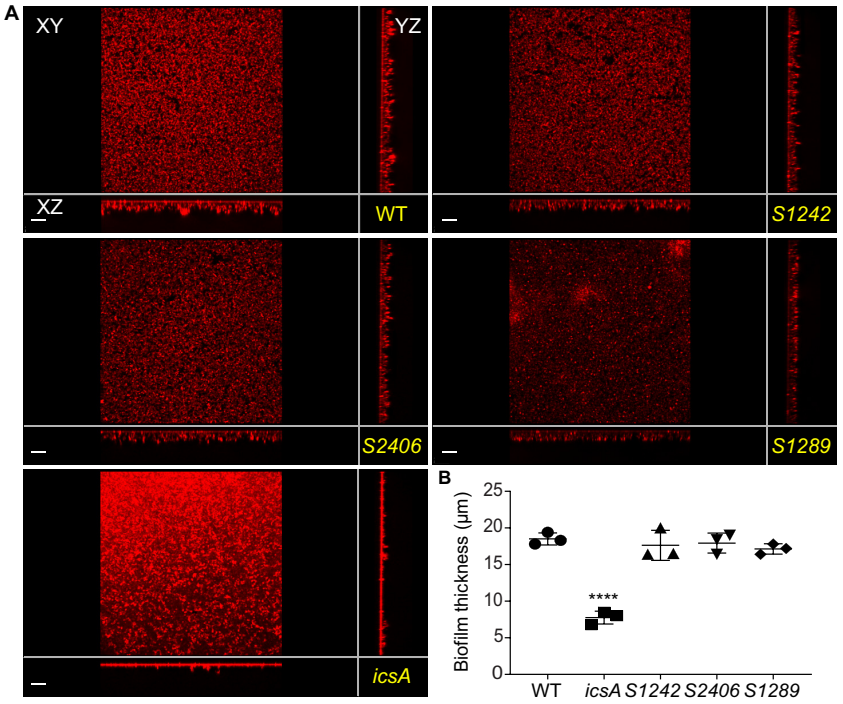

FIG 1 Phenotypic comparison of the biofilms formed by WT and mutant strains. (A) *xy*, *yz*, and *xz* views of the biofilms formed by the WT and mutant strains. Bars, 20 μm. (B) Quantification of biofilm thickness. Symbols in the graph represent the average biofilm thicknesses in 25 fields of view for each biological replicate. One-way ANOVA with Tukey's multiple-comparison test was applied for statistical analysis using GraphPad Prism 7.02. ****, *P* value of $<$0.0001. Error bars represent standard errors of the means from three biological replicates.

in the presence of CA displayed various thickness values across the samples (Fig. S2). To account for this variability, we measured biofilm formation by calculating the total volume of biofilm formed by the *icsA*/pIcsA-Myc rescue strain in TSB with 0.1% DOC (TSB-DOC) or TSB with 0.1% CA (TSB-CA) (Fig. S3). Each bile salt made a significant contribution to biofilm formation compared to TSB control medium (Fig. 4). However,

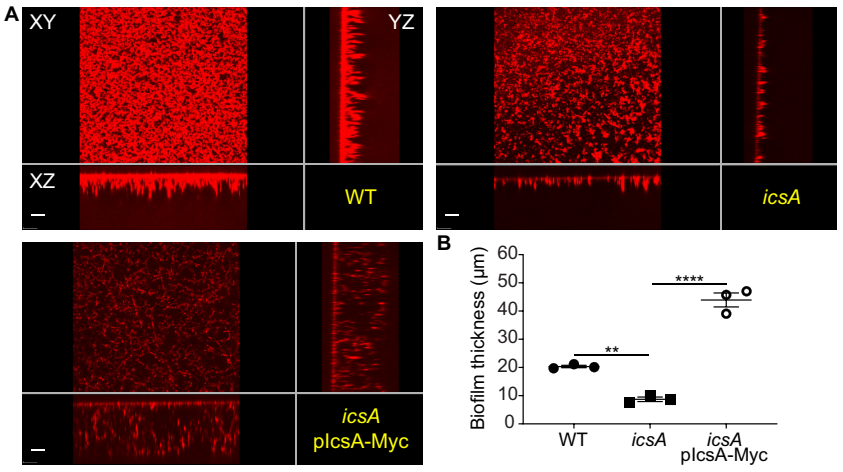

FIG 2 Complementation of the *icsA* mutant strain by IcsA-Myc expression. (A) *xy*, *yz*, and *xz* views from a representative biofilm of each strain. Bars, 10 μm. (B) Quantification of biofilm thickness. Symbols in the graph represent the average biofilm thicknesses in 25 fields of view for each biological replicate. One-way ANOVA with Tukey's multiple-comparison test was applied for statistical analysis using GraphPad Prism 7.02. **, *P* value of $<$0.01; ****, *P* value of $<$0.0001. Error bars represent standard errors of the means from three biological replicates.

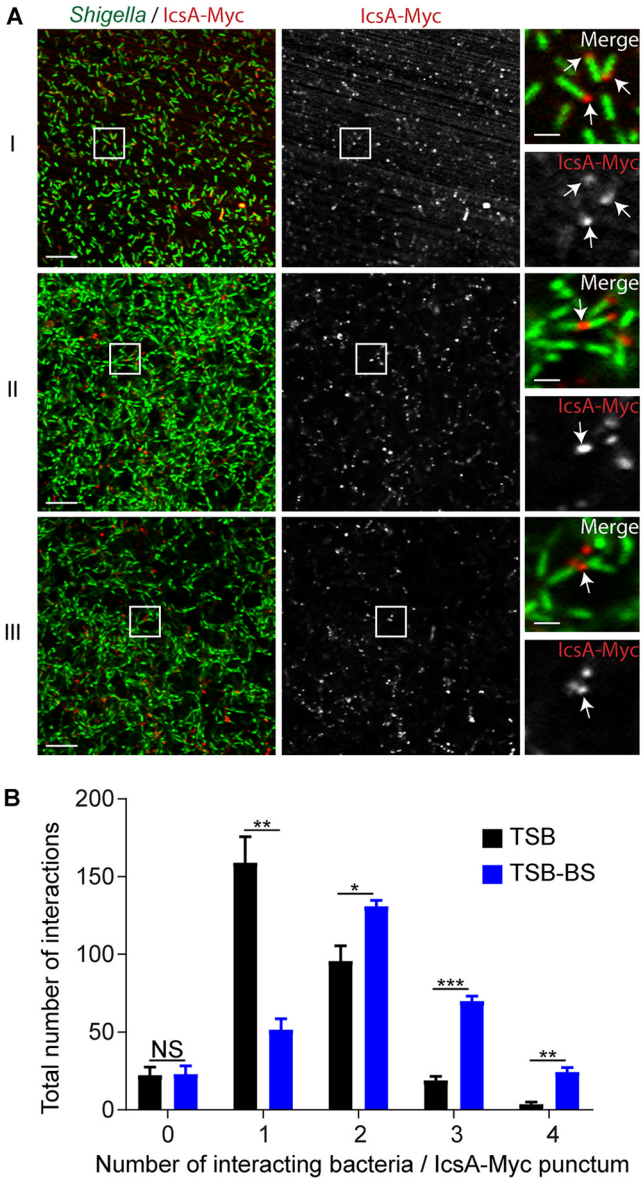

FIG 3 Characterization of IcsA-Myc localization in biofilms. (A) Right panels (bars, 2 μm) showing high-magnification images of *S. flexneri* (green) and IcsA-Myc (red) corresponding to the framed area (white squares) in the representative images of biofilms shown in the left and middle panels (bars, 10 μm). (I) IcsA-Myc polar localization in TSB (white arrows); (II and III) IcsA-Myc localization inside representative TSB-BS biofilms showing polar IcsA-Myc-mediated interactions (white arrows) of two (II) or multiple (III) bacterial cells. (B) Quantification of the number of bacterial cells interacting with IcsA-Myc punctae. Two-way ANOVA was applied for statistical analysis using GraphPad Prism 7.02. NS, not significant; *, *P* value of <0.05; **, *P* value of <0.01; ***, *P* value of <0.001. Error bars represent standard errors of the means from three biological replicates.

the volume of the biofilm formed in the presence of DOC was 3.5-fold higher than the volume formed in the presence of CA (Fig. 4B). These results reveal that DOC, the main bile salt component in the colon, is a potent inducer of *S. flexneri* biofilm formation.

Differential processing of IcsA in the presence of DOC and CA. Under normal growth conditions, the passenger domain of IcsA is released into the extracellular medium through proteolytic cleavage mediated by the serine protease IcsP (Fig. 5A) (50). To examine the potential role of IcsA processing in biofilm formation, we determined IcsA-Myc levels in TSB-DOC and TSB-CA biofilms by Western blot analysis. In the bacterial community that formed after TSB growth, IcsA-Myc appeared as a full-length

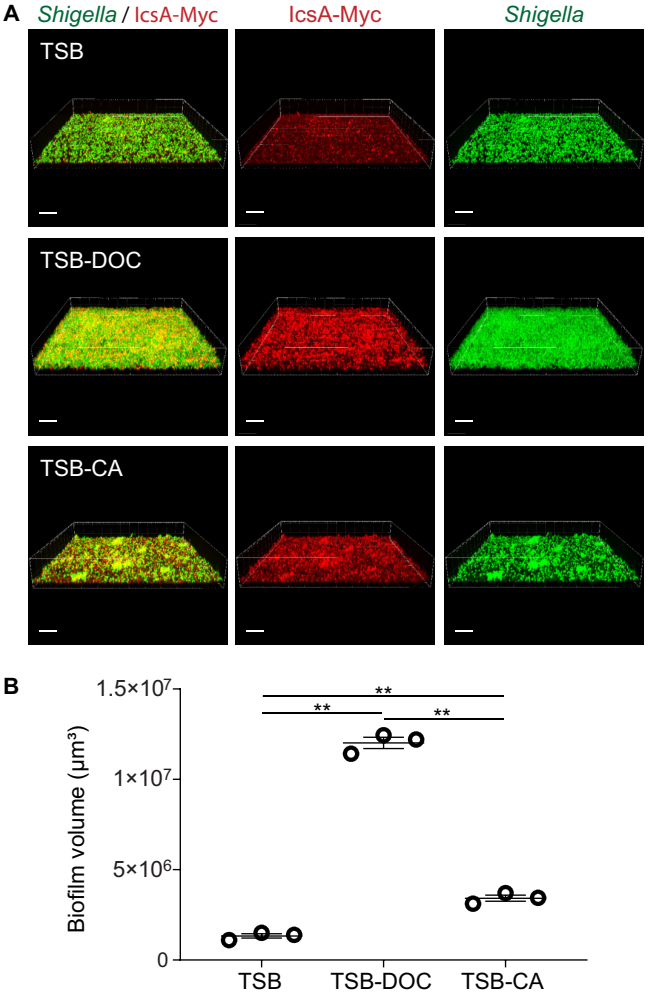

FIG 4 Biofilm formation in the presence of individual bile salt components. (A) Representative three-dimensional (3D) biofilm images. Bars, 30 μm. Green, *Shigella*; Red, IcsA-Myc. (B) Quantification of biofilm volume. Symbols in the graph represent the summation of biofilm volume values in 25 fields of view for each biological replicate. One-way ANOVA with Tukey's multiple-comparison test was applied for statistical analysis using GraphPad Prism 7.02. **, *P* value of $<$0.01. Error bars indicate standard errors of the means from three biological replicates.

protein (120 kDa) or as a processed form corresponding to the cleaved passenger domain (95 kDa) (Fig. 5B). Quantitative analysis showed that IcsA processing was significantly increased in the TSB-CA biofilm (Fig. 5C). We also compared the total amounts of IcsA-Myc species (intact IcsA-Myc plus cleaved IcsA-Myc) in these biofilms. The results (normalized to the value for glyceraldehyde-3-phosphate dehydrogenase [GAPDH]) indicated that total IcsA-Myc levels were similar in TSB, TSB-DOC, and TSB-CA (Fig. 5D). Since biofilm formation was not as robust in TSB-CA (Fig. 4), these results indicate an inverse correlation between IcsA processing and the robustness of biofilm formation.

To rule out the possibility that the observed differential ratios of intact versus cleaved IcsA-Myc in the biofilm may be due to a differential release of the cleaved form in the medium, we also determined IcsA-Myc species in spent medium and floating aggregates. While we did not detect any soluble IcsA-Myc species in the spent medium after pelleting down the floating aggregates, the resulting pellet contained IcsA-Myc species with a ratio similar to that for the corresponding biofilm (Fig. S4). These data indicate that the processed form of IcsA-Myc is a component of the biofilms and floating aggregates that is not released into the medium.

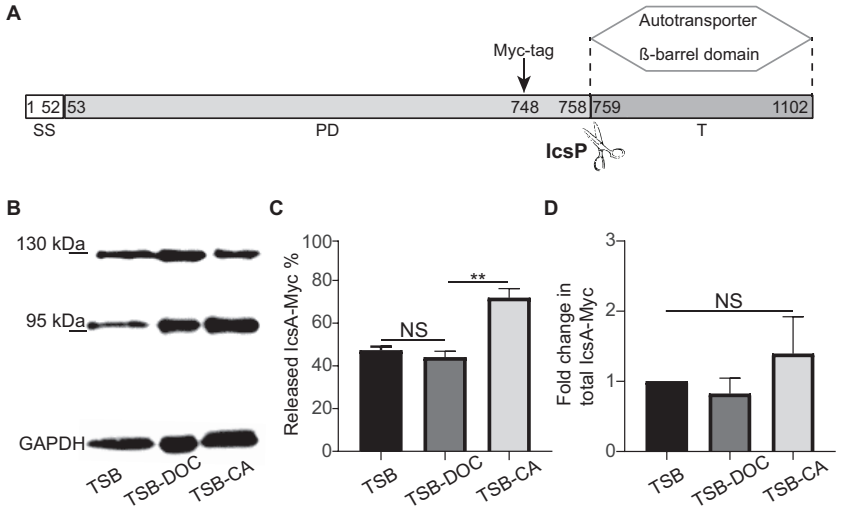

FIG 5 IcsA species within biofilms formed in the presence of individual bile salts. (A) Domain organization of IcsA. Numbers indicate amino acid residues. The IcsP cleavage site between residues 758 and 759 is indicated by scissors. The Myc tag was inserted at position 748, as previously described (21). SS, signal sequence; PD, passenger domain; T, translocator autotransporter β-barrel domain. (B) Western blot analysis of IcsA-Myc species produced in biofilms. A representative blot image shows IcsA-Myc species in surface-associated *Shigella* communities that developed after growth in TSB, TSB-DOC, and TSC-CA media. (C) Quantification of cleaved IcsA-Myc as a percentage of total IcsA-Myc (intact IcsA plus cleaved IcsA). One-way ANOVA with Tukey's multiple-comparison test was applied for statistical analysis using GraphPad Prism 7.02. NS, not significant; **, *P* value of <0.01. Error bars indicate standard errors of the means from three biological replicates. (D) Quantification of total IcsA-Myc levels (intact IcsA plus cleaved IcsA) in TSB-DOC and TSB-CA relative to TSB. One-way ANOVA with Tukey's multiple-comparison test was applied for statistical analysis using GraphPad Prism 7.02. NS, not significant. Error bars indicate standard errors of the means from three biological replicates.

To further assess the contribution of intact and processed IcsA-Myc species, we examined the biofilm formed by the *icsP* mutant, which cannot process IcsA. We found that the *icsP* strain formed a thicker biofilm than the WT strain (*P* value of 0.025) (Fig. 6A and B) and confirmed that it could not process IcsA in biofilms (Fig. 6C). Collectively, these results indicate that full-length IcsA is sufficient for the formation of biofilms (Fig. 6), whose robustness is inversely correlated with the degree of IcsA processing (Fig. 5).

DISCUSSION

Various pathogens undergo biofilm formation in the presence of bile salts. Bile salt components, including CA and DOC, were reported to induce *V. cholerae* biofilm formation via stimulation of exopolysaccharide biosynthesis (27). Similarly, the primary bile salt chenodeoxycholate promotes exopolysaccharide production in *Pseudomonas aeruginosa*, which supports biofilm formation (51). Although physiological levels of bile salts trigger *S. flexneri* biofilm formation (24), *S. flexneri* does not produce common biofilm components such as exopolysaccharides or proteinaceous surface structures (Table 1). Here, we investigated the potential involvement of adhesin-like autotransporter proteins and identified a critical role for IcsA in *S. flexneri* biofilm formation in the presence of bile salts (Fig. 1 and 2).

IcsA is a member of the autotransporter family (52), which is targeted to the bacterial pole, where it is secreted and inserted into the outer membrane (50). The protease IcsP maintains the polarization of full-length IcsA by processing the extracellular domain of the IcsA molecules that diffuse from the pole to the lateral sides of the bacterial cells (50, 53). IcsA polar localization is essential for *S. flexneri* intracellular actin-based motility and cell-to-cell spread. IcsA recruits and activates host components of the actin assembly machinery at the bacterial pole, which propel the bacteria throughout the cytosol (54). Additionally, a recent study reported a role of IcsA adhesion to mammalian cells upon DOC exposure (21). Our results indicate that, in addition to promoting interaction with host cells, IcsA also promotes the development

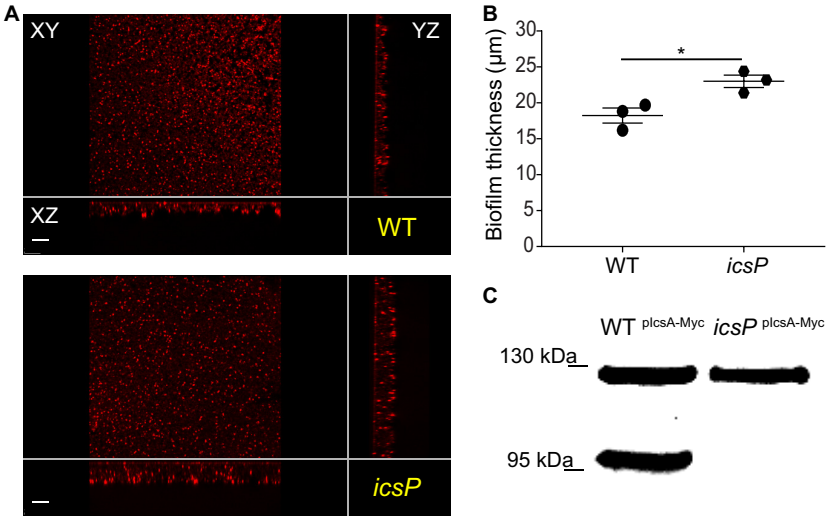

FIG 6 Effect of IcsP-mediated cleavage of IcsA on biofilm formation. (A) *xy*, *yz*, and *xz* views of the biofilms formed by the WT and *icsP* mutant strains. (B) Quantification of biofilm thickness. Symbols in the graph represent the average biofilm thicknesses in 25 fields of view for each biological replicate. Unpaired Student's *t* test was applied for statistical analysis using GraphPad Prism 7.02. *, *P* value of <0.05. Error bars indicate the standard errors of the means from three biological replicates. (C) IcsA-Myc is not cleaved in the *icsP* mutant background. Shown are representative data from Western blot analysis of IcsA-Myc species in the biofilms formed by the WT/pIcsA-Myc ($WT^{IcsA\text{-}Myc}$) and *icsP*/pIcsA-Myc ($icsP^{IcsA\text{-}Myc}$) strains in TSB-BS.

of biofilms by mediating bacterial cell-cell interactions in the presence of bile salts (Fig. 3 and 4). Performing cross-linking experiments and coexpression of mutant versions of IcsA, May et al. demonstrated that IcsA molecules self-associate in the outer membrane (55). IcsA-mediated cell-cell interaction in biofilms may thus reflect the self-association properties of IcsA (Fig. 3). The self-association properties of autotransporter adhesins such as Aida and Ag43 are well documented in *E. coli* (reviewed by Klemm et al. [56]). Aida protein, originally discovered in enteropathogenic *E. coli*, mediates a phenotype of diffuse attachment to HeLa cells by directly binding to an unknown structure(s) on the cell surface (57, 58). In addition to attachment to host cells, Aida facilitates biofilm formation on abiotic surfaces and bacterial autoaggregation under static conditions. The autoaggregation phenotype was connected to intercellular Aida-Aida and Aida-Ag43 interactions (59). Ag43 is another adhesin abundant in *E. coli* species (60). Similar to Aida, Ag43 is also implicated in *E. coli* biofilm development, particularly in glucose-minimal medium (61). Moreover, it can prompt intra- and interspecies bacterial autoaggregation, which stems from Ag43-Ag43 interactions (62, 63). While Aida and Ag43 adhesins do not require external stimuli for self-interactions, our results suggest that bile salts, especially DOC, may stimulate IcsA-IcsA interactions, which lead to aggregative growth and biofilm formation. We speculate that the dependence on bile salts prevents bacterial cell aggregation when bacteria are intracellular, which may interfere with actin-based motility. Accordingly and in agreement with the concept of pathoadaptation, the gene encoding Aida is not present in the *S. flexneri* genome, and *flu* encoding Ag43 is a pseudogene (Table 2).

The exact mechanism(s) supporting IcsA-mediated biofilm formation in the presence of bile salts remains to be elucidated. We tested the effect of individual components on biofilm formation and found that DOC is a more potent biofilm inducer than CA (Fig. 4). DOC displays a higher hydrophobicity and a greater capacity to induce protein aggregation than CA (64). Thus, the stimulatory effect of bile salts on biofilm formation may be related to changes in the IcsA conformation. This is supported by previous work by Brotcke Zumsteg et al. showing that DOC exposure modulates the proteolysis of IcsA by neutrophil elastase (21), suggesting that, through modification of the IcsA conformation, DOC may affect the susceptibility of IcsA to proteases. In

agreement with this notion, our results indicate that IcsA processing by IcsP was decreased in TSB-DOC biofilms compared to TSB-CA biofilms (Fig. 5B and C). We note that the formation of a robust DOC-mediated biofilm in the colon may antagonize the ability of *S. flexneri* to invade epithelial cells. Thus, the regulation of the IcsP-mediated cleavage of IcsA may be critical for pathogenesis through the production of planktonic cells that can readily invade the colonic epithelium. Alternatively, biofilm formation may not contribute to pathogenesis but may facilitate asymptomatic colonization of the human host. It is important to note that *Shigella* isolates from asymptomatic carriers retain virulence traits (65, 66).

In conclusion, our studies reveal a novel extracellular role of IcsA in addition to its roles in actin-based motility and host cell adhesion. These observations are reminiscent of another bacterial factor that supports *Listeria monocytogenes* actin-based motility, ActA, which also promotes bacterial aggregation and biofilm formation (67). We propose that ActA and IcsA have undergone convergent evolution, endowing them with dual functions supporting seemingly unrelated roles in bacterial cell-cell adhesion and actin-based motility during the extracellular and intracellular phases of infection, respectively.

MATERIALS AND METHODS

Bacterial strains and growth conditions. The wild-type *S. flexneri* 2457T strain was used in this study (68). *Escherichia coli* strains such as DH5α, SM10λpir, and Δnic35 were used for cloning, maintenance of pSB890-based constructs, and transformation of *S. flexneri* with pSB890-based constructs by conjugation, respectively. *S. flexneri* and *E. coli* strains were cultured in LB broth (Gentrox) at 37°C overnight on a wheel rotating at 40 rpm. For phenotypic assays, *S. flexneri* frozen stocks (−80°C) were streaked onto LB agar containing 10 μg/ml Congo red dye (Fisher Chemical) (LBCR) and incubated at 37°C overnight to obtain single colonies. When necessary, culture media were supplemented with ampicillin (100 μg/ml), chloramphenicol (10 μg/ml), tetracycline (10 μg/ml), and 100 μg/ml 2,6-diaminopimelic acid (DAP) (Sigma Life Sciences).

Genetic manipulations. Overlap PCRs were performed to construct deletion fragments harboring a chloramphenicol cassette flanked by upstream and downstream regions of the target genes, using the primers listed in Table 3. Deletion fragments and either the pSB890 or pSB890-CAT suicidal vector were digested with the indicated restriction enzymes (New England Biolabs) (Table 3) and ligated with T4 DNA ligase (New England Biolabs). The resulting deletion constructs were confirmed by DNA sequencing. The *S. flexneri* 2457T strain was introduced with the deletion constructs by conjugation. Briefly, 900 μl of a culture of the *E. coli* Δnic35 strain harboring a deletion construct grown overnight was mixed with 300 μl of a culture of the *Shigella* WT strain grown overnight. The mixture was pelleted via centrifugation, and the dense bacterial pellet was spotted onto an LB agar plate supplemented with DAP. The plate was incubated at 30°C for 24 h. After the incubation period, the spot was collected in sterile phosphate-buffered saline (PBS). Serial dilutions were plated onto LB agar supplemented with tetracycline and incubated at 37°C. Colonies were streaked onto LB (without NaCl) agar supplemented with 10% sterile sucrose (Fisher Bioreagents) and chloramphenicol. Finally, mutants were selected on these plates after incubation at 30°C for 24 h.

A pIcsA-Myc construct was generated for phenotypic complementation and IcsA localization in biofilms. We first constructed pBAD18::*icsA* harboring the *icsA* gene, including its promoter region, and subsequently used pBAD::*icsA* as a template to generate the tagged version of IcsA, IcsA-Myc (primers listed in Table 3). The c-Myc tag (EQKLISEEDL) was incorporated into the IcsA autochaperone domain between amino acid residues Ser-748 and Asn-749 and cloned into pBAD18, resulting in pIcsA-Myc, which does not require the addition of arabinose for expression in *S. flexneri*.

Biofilm formation. We used tryptic soy broth (TSB) (Bacto) with 0.4% (wt/vol) bile salts (Fisher Science Education) (TSB-BS), which contains sodium salts of deoxycholic acid and cholic acid for biofilm growth of individual strains. To test the effects of each bile salt on biofilm formation, we used TSB with 0.1% (wt/vol) sodium deoxycholate (catalog number C6750; Sigma-Aldrich) (TSB-DOC) and TSB with 0.1% (wt/vol) sodium cholate (catalog number C6445; Sigma Life Sciences) (TSB-CA) as biofilm growth media. To maintain the pIcsA-Myc construct, biofilm growth medium was supplemented with ampicillin. The glass coverslips were coated with poly-D-lysine (Cultrex) overnight at room temperature in 24-well plates prior to biofilm growth. Biofilms were formed at 37°C for 24 h on 12-mm microscope glass coverslips (Fisherbrand) immersed in biofilm growth medium in 24-well plates. Briefly, fresh *S. flexneri* Congo red-positive colonies grown on LBCR plates with appropriate antibiotics were transferred to LB medium (50 to 150 μl), and these bacterial suspensions were then immediately diluted in biofilm growth medium at a 1:100 ratio. Five hundred microliters of biofilm growth medium seeded with *S. flexneri* was transferred to 24-well plates with poly-D-lysine-coated coverslips. The 24-well plates were sealed with parafilm and incubated at 37°C for biofilm growth. After 24 h, an equal volume of an 8% paraformaldehyde (Electron Microscopy Sciences) solution was directly added to the cultures for overnight fixation at 4°C. Fixed spent medium was aspirated gently, and the fixed biofilms on the coverslips were washed twice with PBS. Then coverslips were incubated with unconjugated rabbit antibody against *Shigella* spp. (ViroStat) and then with Alexa Fluor 594 (AF-594) goat anti-rabbit antibody (Life Technologies) at room

TABLE 3 Primers used in the study

DNA manipulation and primer name	Sequence (5′→3′)[a]
S2406 deletion	
5S2406	TGAGATCCAGCAAGATCACGTCG
3S2406	CTAAGGAGGATATTCATATGTTGATGCATTGAGCTTTCATCCTATG
5S2406-CAT	CATAGGATGAAAGCTCAATGCATCAACATATGAATATCCTCCTTAG
3S2406-CAT	CTGTTATCAGAACGTCCAGACCACGTGTAGGCTGGAGCTGCTTC
5CAT-S2406	GAAGCAGCTCCAGCCTACACGTGGTCTGGACGTTCTGATAACAG
3CAT-S2406	CGCAAGGTCAGGATTTGTTCAACC
S1242 deletion	
5S1242_NotI	AATT**GCGGCCGC**GACAGGATTGCCATTAGTAGCATG
3S1242_blunt	AATTCATTGCGTTAACAGTCAATGACAC
5S1242-CAT	GCAGGGTAAAAACACGATTGTCACCATATGAATATCCTCCTTAG
3S1242-CAT	CTAAGGAGGATATTCATATGGTGACAATCGTGTTTTTACCCTGC
5CAT-S1242	CGAAGCAGCTCCAGCCTACACGGTGGGCCTGAAATATAAGTTC
3CAT-S1242	GAACTTATATTTCAGGCCCACCGTGTAGGCTGGAGCTGCTTCG
icsA deletion	
5icsA-UP-SacI	AATT**GAGCTC**CAGGGCGTGTTGATGTCCTGC
3icsA-UP-XhoI	AATT**CTCGAG**GTAAGTGGTTGATAAACCCCTG
5icsA-DOWN-SacI	AATT**GAGCTC**CAGGGCGTGTTGATGTCCTGC
3icsA-DOWN-BamHI	AATT**GGATCC**CGACCCCGTACTGCTCACGCA
S1289 deletion	
5S1289-UP-NotI	AATT**GCGGCCGC**GGCTTTATCCGTGCACAAACC
3S1289-UP-XhoI	AATT**CTCGAG**CCACTCCTATATAGTACCCAGG
5S1289-DOWN-SacI	AATT**GAGCTC**CAACGGAGGATATCGCTTCAGC
3S1289-DOWN-PstI	AATT**CTGCAG**CCTGTCCTGCTTTGTGGAGAAG
icsP deletion	
5icsP-UP-NotI	ATAT**GCGGCCGC**GATTAGTCCTTAATCGGACAACCAC
3icsP-UP-XhoI	ATAT**CTCGAG**GATCTTCTTACTTTATAAGATAAACGTCAA
5icsP-DOWN-SacI	GGG**GAGCTC**ATTGGTTCACCGAGTTGATTACGTT
3icsP-DOWN-PstI	GGG**CTGCAG**GTCCCTGATAGCACTGTTCCATCA
IcsA expression	
FW-SmaI	ATTA**CCCGGG**GGTTAGTTATGTTTGATGTCTGC
REV-SalI	ATTA**GTCGAC**CCTCGTACAGAACTACTCAAGTCC
IcsA-Myc expression	
5IcsA-UP-BplI	GGCCATGCGTCTGGTATTACC
3IcsA-Myc-748aa	AAGATCTTCTTCAGAAATAAGTTTTTGTTCGCTCATCTGTTTTGATTCTTGA
5IcsA-Myc-748aa	GAACAAAAACTTATTTCTGAAGAAGATCTTAATCAAGAGTCTACTCAAAT
3IcsA-DOWN-BbsI	CCATAAGCTCCCATAATACCC

[a]Restriction sites are in boldface type.

temperature (each 75 min). The coverslips were mounted onto microscope slides with ProLong Gold antifade reagent (Invitrogen). Biofilm images were acquired with a Leica DMI 8 spinning-disc 474 confocal microscope controlled by iQ software (Andor).

IcsA localization in biofilms. The *icsA*/pIcsA-Myc strain was used for biofilm growth in TSB, TSB-DOC, TSB-CA, and TSB-BS, as mentioned above. Biofilms on the coverslips were incubated with PBS containing the mouse monoclonal antibody for the Myc tag (Cell Signaling) (1:1,000 dilution) at room temperature for 75 min. Coverslips were washed twice with PBS, and secondary staining was carried out with 1× PBS–0.1% Triton X-100 containing SYTOX green (Invitrogen) (1:10,000 dilution) and secondary goat anti-mouse AF-594 antibody at room temperature for 75 min. The coverslips were mounted onto microscope slides with ProLong Gold antifade reagent (Invitrogen) following the final wash with PBS. Biofilm images were acquired with a Leica DMI 8 spinning-disc 474 confocal microscope controlled by iQ software (Andor).

Biofilm measurements. Biofilms were quantified in two different ways, by measuring biofilm thickness (micrometers) and the total biofilm volume on the glass surface (cubic micrometers). Quantification of biofilm thickness was performed by defining the bottom and the top layers of each biofilm with the Slice tool of Imaris imaging software. Experiments were carried out in triplicate, and in each replicate, 25 random fields (technical repeats) on a glass coverslip were acquired for biofilm thickness measurements. Due to irregular biofilm structures formed in TSB-CA medium, we measured the volume of biofilms instead of thickness. After fixation of biofilms formed by the *icsA*/pIcsA-Myc strain, 25 random fields were acquired for each medium (TSB, TSB-DOC, and TSB-CA). Next, the biofilm volume values of 25

fields were estimated using the Surface function of Imaris imaging software. We summed the estimated values to obtain a total biofilm volume value that represents the biofilm formed in each medium. One-way analysis of variance (ANOVA) with Tukey's multiple-comparison test and an unpaired Student *t* test were performed for statistical analysis using GraphPad Prism 7.02.

Western blotting. In parallel to biofilm volume measurements, we also prepared samples from another set of coverslips for assessment of IcsA-Myc levels in biofilms of the *icsA*/pIcsA-Myc strain that developed during growth in TSB, TSB-DOC, and TSB-CA media. After biofilm growth, spent media were removed from the wells, and coverslips were then washed gently with PBS twice. Samples were collected from the surface of coverslips with 100 μl of sample buffer (2× SDS gel loading buffer with 100 mM dithiothreitol [DTT]). To assess IcsA-Myc species in biofilm spent media, floating aggregates were collected by centrifugation at 10,000 × *g* for 10 min at 4°C. Pellets were immediately treated with sample buffer. Clear supernatants were filter sterilized with a 0.22-μm membrane filter unit (Millex-GS). Soluble proteins were precipitated with 10% trichloroacetic acid (69). Protein samples were first separated by SDS-PAGE and then transferred to nitrocellulose membranes (100 V for 1 h at 4°C). Membranes were blocked with PBS containing 0.1% Tween 20 and 5% bovine serum albumin (BSA) at room temperature for 1 h and then blotted with primary mouse monoclonal antibody for the Myc tag (Cell Signaling) (overnight at 4°C) and horseradish peroxidase (HRP)-conjugated goat anti-mouse IgG (1:10,000) secondary antibody (Jackson) (1 h at room temperature). Protein bands were developed with Amersham ECL Western blotting detection reagents. The exact same procedure was conducted to determine IcsA-Myc species in the biofilms formed by the *icsP*/pIcsA-Myc and WT/pIcsA-Myc strains.

SUPPLEMENTAL MATERIAL

Supplemental material for this article may be found at https://doi.org/10.1128/IAI.00861-18.

SUPPLEMENTAL FILE 1, PDF file, 0.3 MB.

ACKNOWLEDGMENTS

We thank members of the Agaisse laboratory for discussions and Melissa Kendall for providing the GAPDH antibody.

This work was supported by National Institutes of Health grants T32AI055432 (C.P.H.) and R01AI073904 (H.A.).

REFERENCES

1. GBD Diarrhoeal Diseases Collaborators. 2017. Estimates of global, regional, and national morbidity, mortality, and aetiologies of diarrhoeal diseases: a systematic analysis for the Global Burden of Disease Study 2015. Lancet Infect Dis 17:909–948. https://doi.org/10.1016/S1473-3099(17)30276-1.
2. Anderson M, Sansonetti PJ, Marteyn BS. 2016. Shigella diversity and changing landscape: insights for the twenty-first century. Front Cell Infect Microbiol 6:45. https://doi.org/10.3389/fcimb.2016.00045.
3. Livio S, Strockbine NA, Panchalingam S, Tennant SM, Barry EM, Marohn ME, Antonio M, Hossain A, Mandomando I, Ochieng JB, Oundo JO, Qureshi S, Ramamurthy T, Tamboura B, Adegbola RA, Hossain MJ, Saha D, Sen S, Faruque ASG, Alonso PL, Breiman RF, Zaidi AKM, Sur D, Sow SO, Berkeley LY, O'Reilly CE, Mintz ED, Biswas K, Cohen D, Farag TH, Nasrin D, Wu Y, Blackwelder WC, Kotloff KL, Nataro JP, Levine MM. 2014. Shigella isolates from the global enteric multicenter study inform vaccine development. Clin Infect Dis 59:933–941. https://doi.org/10.1093/cid/ciu468.
4. Kotloff KL, Winickoff JP, Ivanoff B, Clemens JD, Swerdlow DL, Sansonetti PJ, Adak GK, Levine MM. 1999. Global burden of Shigella infections: implications for vaccine development and implementation of control strategies. Bull World Health Organ 77:651–666.
5. DuPont HL, Levine MM, Hornick RB, Formal SB. 1989. Inoculum size in shigellosis and implications for expected mode of transmission. J Infect Dis 159:1126–1128. https://doi.org/10.1093/infdis/159.6.1126.
6. Scallan E, Hoekstra RM, Angulo FJ, Tauxe RV, Widdowson M-A, Roy SL, Jones JL, Griffin PM. 2011. Foodborne illness acquired in the United States—major pathogens. Emerg Infect Dis 17:7–15. https://doi.org/10.3201/eid1701.091101p1.
7. Schroeder GN, Hilbi H. 2008. Molecular pathogenesis of Shigella spp.: controlling host cell signaling, invasion, and death by type III secretion. Clin Microbiol Rev 21:134–156. https://doi.org/10.1128/CMR.00032-07.
8. Mattock E, Blocker AJ. 2017. How do the virulence factors of Shigella work together to cause disease? Front Cell Infect Microbiol 7:64. https://doi.org/10.3389/fcimb.2017.00064.
9. Buchrieser C, Glaser P, Rusniok C, Nedjari H, D'Hauteville H, Kunst F, Sansonetti P, Parsot C. 2000. The virulence plasmid pWR100 and the repertoire of proteins secreted by the type III secretion apparatus of Shigella flexneri. Mol Microbiol 38:760–771. https://doi.org/10.1046/j.1365-2958.2000.02179.x.
10. Venkatesan MM, Goldberg MB, Rose DJ, Grotbeck EJ, Burland V, Blattner FR. 2001. Complete DNA sequence and analysis of the large virulence plasmid of Shigella flexneri. Infect Immun 69:3271–3285. https://doi.org/10.1128/IAI.69.5.3271-3285.2001.
11. Agaisse H. 2016. Molecular and cellular mechanisms of Shigella flexneri dissemination. Front Cell Infect Microbiol 6:29. https://doi.org/10.3389/fcimb.2016.00029.
12. Marteyn BS, Gazi AD, Sansonetti PJ. 2012. Shigella: a model of virulence regulation in vivo. Gut Microbes 3:104–120. https://doi.org/10.4161/gmic.19325.
13. Begley M, Gahan CGM, Hill C. 2005. The interaction between bacteria and bile. FEMS Microbiol Rev 29:625–651. https://doi.org/10.1016/j.femsre.2004.09.003.
14. Chiang JYL. 2009. Bile acids: regulation of synthesis. J Lipid Res 50:1955–1966. https://doi.org/10.1194/jlr.R900010-JLR200.
15. Hofmann AF, Hagey LR. 2008. Bile acids: chemistry, pathochemistry, biology, pathobiology, and therapeutics. Cell Mol Life Sci 65:2461–2483. https://doi.org/10.1007/s00018-008-7568-6.
16. Ridlon JM, Kang D-J, Hylemon PB. 2006. Bile salt biotransformations by human intestinal bacteria. J Lipid Res 47:241–259. https://doi.org/10.1194/jlr.R500013-JLR200.
17. Urdaneta V, Casadesús J. 2017. Interactions between bacteria and bile salts in the gastrointestinal and hepatobiliary tracts. Front Med (Lausanne) 4:163. https://doi.org/10.3389/fmed.2017.00163.
18. Sistrunk JR, Nickerson KP, Chanin RB, Rasko DA, Faherty CS. 2016. Survival of the fittest: how bacterial pathogens utilize bile to enhance infection. Clin Microbiol Rev 29:819–836. https://doi.org/10.1128/CMR.00031-16.
19. Pope LM, Reed KE, Payne SM. 1995. Increased protein secretion and adherence to HeLa cells by Shigella spp. following growth in the presence of bile salts. Infect Immun 63:3642–3648.

20. Faherty CS, Redman JC, Rasko DA, Barry EM, Nataro JP. 2012. Shigella flexneri effectors OspE1 and OspE2 mediate induced adherence to the colonic epithelium following bile salts exposure. Mol Microbiol 85:107–121. https://doi.org/10.1111/j.1365-2958.2012.08092.x.
21. Brotcke Zumsteg A, Goosmann C, Brinkmann V, Morona R, Zychlinsky A. 2014. IcsA is a Shigella flexneri adhesin regulated by the type III secretion system and required for pathogenesis. Cell Host Microbe 15:435–445. https://doi.org/10.1016/j.chom.2014.03.001.
22. Olive AJ, Kenjale R, Espina M, Moore DS, Picking WL, Picking WD. 2007. Bile salts stimulate recruitment of IpaB to the Shigella flexneri surface, where it colocalizes with IpaD at the tip of the type III secretion needle. Infect Immun 75:2626–2629. https://doi.org/10.1128/IAI.01599-06.
23. Dickenson NE, Zhang L, Epler CR, Adam PR, Picking WL, Picking WD. 2011. Conformational changes in IpaD from Shigella flexneri upon binding bile salts provide insight into the second step of type III secretion. Biochemistry 50:172–180. https://doi.org/10.1021/bi101365f.
24. Nickerson KP, Chanin RB, Sistrunk JR, Rasko DA, Fink PJ, Barry EM, Nataro JP, Faherty CS. 2017. Analysis of Shigella flexneri resistance, biofilm formation, and transcriptional profile in response to bile salts. Infect Immun 85:e01067-16. https://doi.org/10.1128/IAI.01067-16.
25. Prouty AM, Schwesinger WH, Gunn JS. 2002. Biofilm formation and interaction with the surfaces of gallstones by Salmonella spp. Infect Immun 70:2640–2649. https://doi.org/10.1128/IAI.70.5.2640-2649.2002.
26. Crawford RW, Gibson DL, Kay WW, Gunn JS. 2008. Identification of a bile-induced exopolysaccharide required for Salmonella biofilm formation on gallstone surfaces. Infect Immun 76:5341–5349. https://doi.org/10.1128/IAI.00786-08.
27. Hung DT, Zhu J, Sturtevant D, Mekalanos JJ. 2006. Bile acids stimulate biofilm formation in Vibrio cholerae. Mol Microbiol 59:193–201. https://doi.org/10.1111/j.1365-2958.2005.04846.x.
28. O'Toole G, Kaplan HB, Kolter R. 2000. Biofilm formation as microbial development. Annu Rev Microbiol 54:49–79. https://doi.org/10.1146/annurev.micro.54.1.49.
29. De la Fuente-Núñez C, Reffuveille F, Fernández L, Hancock REW. 2013. Bacterial biofilm development as a multicellular adaptation: antibiotic resistance and new therapeutic strategies. Curr Opin Microbiol 16:580–589. https://doi.org/10.1016/j.mib.2013.06.013.
30. Hall-Stoodley L, Costerton JW, Stoodley P. 2004. Bacterial biofilms: from the natural environment to infectious diseases. Nat Rev Microbiol 2:95–108. https://doi.org/10.1038/nrmicro821.
31. Flemming HC, Wingender J, Szewzyk U, Steinberg P, Rice SA, Kjelleberg S. 2016. Biofilms: an emergent form of bacterial life. Nat Rev Microbiol 14:563–575. https://doi.org/10.1038/nrmicro.2016.94.
32. Flemming HC, Wingender J. 2010. The biofilm matrix. Nat Rev Microbiol 8:623–633. https://doi.org/10.1038/nrmicro2415.
33. Hazen TH, Leonard SR, Lampel KA, Lacher DW, Maurelli AT, Rasko DA. 2016. Investigating the relatedness of enteroinvasive Escherichia coli to other E. coli and Shigella isolates by using comparative genomics. Infect Immun 84:2362–2371. https://doi.org/10.1128/IAI.00350-16.
34. Chattaway MA, Schaefer U, Tewolde R, Dallman TJ, Jenkins C. 2017. Identification of Escherichia coli and Shigella species from whole-genome sequences. J Clin Microbiol 55:616–623. https://doi.org/10.1128/JCM.01790-16.
35. Bliven KA, Maurelli AT. 2012. Antivirulence genes: insights into pathogen evolution through gene loss. Infect Immun 80:4061–4070. https://doi.org/10.1128/IAI.00740-12.
36. Yang F, Yang J, Zhang X, Chen L, Jiang Y, Yan Y, Tang X, Wang J, Xiong Z, Dong J, Xue Y, Zhu Y, Xu X, Sun L, Chen S, Nie H, Peng J, Xu J, Wang Y, Yuan Z, Wen Y, Yao Z, Shen Y, Qiang B, Hou Y, Yu J, Jin Q. 2005. Genome dynamics and diversity of Shigella species, the etiologic agents of bacillary dysentery. Nucleic Acids Res 33:6445–6458. https://doi.org/10.1093/nar/gki954.
37. Al Mamun AA, Tominaga A, Enomoto M. 1996. Detection and characterization of the flagellar master operon in the four Shigella subgroups. J Bacteriol 178:3722–3726. https://doi.org/10.1128/jb.178.13.3722-3726.1996.
38. Bravo V, Puhar A, Sansonetti P, Parsot C, Toro CS. 2015. Distinct mutations led to inactivation of type 1 fimbriae expression in Shigella spp. PLoS One 10:e0121785. https://doi.org/10.1371/journal.pone.0121785.
39. Sakellaris H, Hannink NK, Rajakumar K, Bulach D, Hunt M, Sasakawa C, Adler B. 2000. Curli loci of Shigella spp. Infect Immun 68:3780–3783. https://doi.org/10.1128/IAI.68.6.3780-3783.2000.
40. Whitney JC, Howell PL. 2013. Synthase-dependent exopolysaccharide secretion in Gram-negative bacteria. Trends Microbiol 21:63–72. https://doi.org/10.1016/j.tim.2012.10.001.
41. Römling U, Galperin MY. 2015. Bacterial cellulose biosynthesis: diversity of operons, subunits, products, and functions. Trends Microbiol 23:545–557. https://doi.org/10.1016/j.tim.2015.05.005.
42. Caboni M, Pédron T, Rossi O, Goulding D, Pickard D, Citiulo F, MacLennan CA, Dougan G, Thomson NR, Saul A, Sansonetti PJ, Gerke C. 2015. An O antigen capsule modulates bacterial pathogenesis in Shigella sonnei. PLoS Pathog 11:e1004749. https://doi.org/10.1371/journal.ppat.1004749.
43. Berne C, Ducret A, Hardy GG, Brun YV. 2015. Adhesins involved in attachment to abiotic surfaces by Gram-negative bacteria. Microbiol Spectr 3(4):MB-0018-2015. https://doi.org/10.1128/microbiolspec.MB-0018-2015.
44. Vo JL, Martínez Ortiz GC, Subedi P, Keerthikumar S, Mathivanan S, Paxman JJ, Heras B. 2017. Autotransporter adhesins in Escherichia coli pathogenesis. Proteomics 17:1600431. https://doi.org/10.1002/pmic.201600431.
45. Celik N, Webb CT, Leyton DL, Holt KE, Heinz E, Gorrell R, Kwok T, Naderer T, Strugnell RA, Speed TP, Teasdale RD, Likić VA, Lithgow T. 2012. A bioinformatic strategy for the detection, classification and analysis of bacterial autotransporters. PLoS One 7:e43245. https://doi.org/10.1371/journal.pone.0043245.
46. Drobnak I, Braselmann E, Chaney JL, Leyton DL, Bernstein HD, Lithgow T, Luirink J, Nataro JP, Clark PL. 2015. Of linkers and autochaperones: an unambiguous nomenclature to identify common and uncommon themes for autotransporter secretion. Mol Microbiol 95:1–16. https://doi.org/10.1111/mmi.12838.
47. Leyton DL, Rossiter AE, Henderson IR. 2012. From self sufficiency to dependence: mechanisms and factors important for autotransporter biogenesis. Nat Rev Microbiol 10:213–225. https://doi.org/10.1038/nrmicro2733.
48. Henderson IR, Navarro-Garcia F, Desvaux M, Fernandez RC, Ala'Aldeen D. 2004. Type V protein secretion pathway: the autotransporter story. Microbiol Mol Biol Rev 68:692–744. https://doi.org/10.1128/MMBR.68.4.692-744.2004.
49. Goldberg MB, Barzu O, Parsot C, Sansonetti PJ. 1993. Unipolar localization and ATPase activity of IcsA, a Shigella flexneri protein involved in intracellular movement. J Bacteriol 175:2189–2196. https://doi.org/10.1128/jb.175.8.2189-2196.1993.
50. Steinhauer J, Agha R, Pham T, Varga AW, Goldberg MB. 1999. The unipolar Shigella surface protein IcsA is targeted directly to the bacterial old pole: IcsP cleavage of IcsA occurs over the entire bacterial surface. Mol Microbiol 32:367–377. https://doi.org/10.1046/j.1365-2958.1999.01356.x.
51. Reen FJ, Flynn S, Woods DF, Dunphy N, Chróinín MN, Mullane D, Stick S, Adams C, O'Gara F. 2016. Bile signalling promotes chronic respiratory infections and antibiotic tolerance. Sci Rep 6:29768. https://doi.org/10.1038/srep29768.
52. Henderson IR, Navarro-Garcia F, Nataro JP. 1998. The great escape: structure and function of the autotransporter proteins. Trends Microbiol 6:370–378. https://doi.org/10.1016/S0966-842X(98)01318-3.
53. Robbins JR, Monack D, McCallum SJ, Vegas A, Pham E, Goldberg MB, Theriot JA. 2001. The making of a gradient: IcsA (VirG) polarity in Shigella flexneri. Mol Microbiol 41:861–872.
54. Bernardini ML, Mounier J, d'Hauteville H, Coquis-Rondon M, Sansonetti PJ. 1989. Identification of *icsA*, a plasmid locus of *Shigella flexneri* that governs bacterial intra- and intercellular spread through interaction with F-actin. Proc Natl Acad Sci U S A 86:3867–3871. https://doi.org/10.1073/pnas.86.10.3867.
55. May KL, Grabowicz M, Polyak SW, Morona R. 2012. Self-association of the Shigella flexneri IcsA autotransporter protein. Microbiology 158:1874–1883. https://doi.org/10.1099/mic.0.056465-0.
56. Klemm P, Vejborg RM, Sherlock O. 2006. Self-associating autotransporters, SAATs: functional and structural similarities. Int J Med Microbiol 296:187–195. https://doi.org/10.1016/j.ijmm.2005.10.002.
57. Benz I, Schmidt MA. 1989. Cloning and expression of an adhesin (AIDA-I) involved in diffuse adherence of enteropathogenic Escherichia coli. Infect Immun 57:1506–1511.
58. Benz I, Schmidt MA. 1992. Isolation and serologic characterization of AIDA-I, the adhesin mediating the diffuse adherence phenotype of the diarrhea-associated Escherichia coli strain 2787 (O126:H27). Infect Immun 60:13–18.
59. Sherlock O, Schembri MA, Reisner A, Klemm P. 2004. Novel roles for the

AIDA adhesin from diarrheagenic Escherichia coli: cell aggregation and biofilm formation. J Bacteriol 186:8058–8065. https://doi.org/10.1128/JB.186.23.8058-8065.2004.
60. van der Woude MW, Henderson IR. 2008. Regulation and function of Ag43 (Flu). Annu Rev Microbiol 62:153–169. https://doi.org/10.1146/annurev.micro.62.081307.162938.
61. Danese PN, Pratt LA, Dove SL, Kolter R. 2000. The outer membrane protein, antigen 43, mediates cell-to-cell interactions within Escherichia coli biofilms. Mol Microbiol 37:424–432. https://doi.org/10.1046/j.1365-2958.2000.02008.x.
62. Kjærgaard K, Schembri MA, Hasman H, Klemm P. 2000. Antigen 43 from Escherichia coli induces inter- and intraspecies cell aggregation and changes in colony morphology of Pseudomonas fluorescens. J Bacteriol 182:4789–4796. https://doi.org/10.1128/JB.182.17.4789-4796.2000.
63. Hasman H, Chakraborty T, Klemm P. 1999. Antigen-43-mediated autoaggregation of Escherichia coli is blocked by fimbriation. J Bacteriol 181:4834–4841.
64. Cremers CM, Knoefler D, Vitvitsky V, Banerjee R, Jakob U. 2014. Bile salts act as effective protein-unfolding agents and instigators of disulfide stress in vivo. Proc Natl Acad Sci U S A 111:E1610–E1619. https://doi.org/10.1073/pnas.1401941111.
65. Haider K, Huq MI, Samadi AR, Ahmad K. 1986. Plasmid characterization of Shigella spp. isolated from children with shigellosis and asymptomatic excretors. J Antimicrob Chemother 16:691–698. https://doi.org/10.1093/jac/16.6.691.
66. Ghosh S, Pazhani GP, Niyogi SK, Nataro JP, Ramamurthy T. 2014. Genetic characterization of Shigella spp. isolated from diarrhoeal and asymptomatic children. J Med Microbiol 63:903–910. https://doi.org/10.1099/jmm.0.070912-0.
67. Travier L, Guadagnini S, Gouin E, Dufour A, Chenal-Francisque V, Cossart P, Olivo-Marin J-C, Ghigo J-M, Disson O, Lecuit M. 2013. ActA promotes Listeria monocytogenes aggregation, intestinal colonization and carriage. PLoS Pathog 9:e1003131. https://doi.org/10.1371/journal.ppat.1003131.
68. Labrec EH, Schneider H, Magnani TJ, Formal SB. 1964. Epithelial cell penetration as an essential step in the pathogenesis of bacillary dysentery. J Bacteriol 88:1503–1518.
69. Reinhardt J, Kolbe M. 2014. Secretion assay in Shigella flexneri. Bio Protoc 4:e1302.
70. Serra DO, Richter AM, Hengge R. 2013. Cellulose as an architectural element in spatially structured Escherichia coli biofilms. J Bacteriol 195:5540–5554. https://doi.org/10.1128/JB.00946-13.
71. Hung C, Zhou Y, Pinkner JS, Dodson KW, Crowley JR, Heuser J, Chapman MR, Hadjifrangiskou M, Henderson JP, Hultgren SJ. 2013. Escherichia coli biofilms have an organized and complex extracellular matrix structure. mBio 4:e00645-13. https://doi.org/10.1128/mBio.00645-13.
72. McCrate OA, Zhou X, Reichhardt C, Cegelski L. 2013. Sum of the parts: composition and architecture of the bacterial extracellular matrix. J Mol Biol 425:4286–4294. https://doi.org/10.1016/j.jmb.2013.06.022.
73. Wang X, Preston JF, III, Romeo T. 2004. The pgaABCD locus of Escherichia coli promotes the synthesis of a polysaccharide adhesin required for biofilm formation. J Bacteriol 186:2724–2734. https://doi.org/10.1128/JB.186.9.2724-2734.2004.
74. Danese PN, Pratt LA, Kolter R. 2000. Exopolysaccharide production is required for development of *Escherichia coli* K-12 biofilm architecture. J Bacteriol 182:3593–3596. https://doi.org/10.1128/JB.182.12.3593-3596.2000.
75. Anderson GG, Goller CC, Justice S, Hultgren SJ, Seed PC. 2010. Polysaccharide capsule and sialic acid-mediated regulation promote biofilm-like intracellular bacterial communities during cystitis. Infect Immun 78:963–975. https://doi.org/10.1128/IAI.00925-09.
76. Pratt LA, Kolter R. 1998. Genetic analysis of Escherichia coli biofilm formation: roles of flagella, motility, chemotaxis and type I pili. Mol Microbiol 30:285–293. https://doi.org/10.1046/j.1365-2958.1998.01061.x.
77. Serra DO, Richter AM, Klauck G, Mika F, Hengge R. 2013. Microanatomy at cellular resolution and spatial order of physiological differentiation in a bacterial biofilm. mBio 4:e00103-13. https://doi.org/10.1128/mBio.00103-13.
78. Wright KJ, Seed PC, Hultgren SJ. 2007. Development of intracellular bacterial communities of uropathogenic Escherichia coli depends on type 1 pili. Cell Microbiol 9:2230–2241. https://doi.org/10.1111/j.1462-5822.2007.00952.x.
79. Moreira CG, Palmer K, Whiteley M, Sircili MP, Trabulsi LR, Castro AFP, Sperandio V. 2006. Bundle-forming pili and EspA are involved in biofilm formation by enteropathogenic Escherichia coli. J Bacteriol 188:3952–3961. https://doi.org/10.1128/JB.00177-06.